

# Structural and Energetic Relations between $\beta$ Turns

KERSTIN MÖHLE,<sup>1</sup> MARTIN GUßMANN,<sup>1</sup> HANS-JÖRG HOFMANN<sup>2</sup>

<sup>1</sup>Institut für Physikalische und Theoretische Chemie, Institut für Analytische Chemie, Fakultät für Chemie und Mineralogie, Universität Leipzig, Leipzig, Germany

<sup>2</sup>Institut für Biochemie, Fakultät für Biowissenschaften, Pharmazie und Psychologie, Universität Leipzig, Talstraße 33, D-04103 Leipzig, Germany

Received 6 December 1996; accepted 3 February 1997

**ABSTRACT:** A systematic quantum chemical study on the structure and stability of the major types of  $\beta$ -turn structures in peptides and proteins was performed at different levels of *ab initio* MO theory (MP2/6-31G\*, HF/6-31G\*, HF/3-21G) considering model turns of the general type  $\text{Ac}-\text{X}_{\text{aa}}-\text{Y}_{\text{aa}}-\text{NHCH}_3$  with the amino acids glycine, L- and D-alanine, aminoisobutyric acid, and L-proline. The influence of correlation effects, zero-point vibration energies, thermal energies, and entropies on the turn formation was examined. Solvent effects on the turn stabilities were estimated employing quantum chemical continuum approaches (Onsager's self-consistent reaction field and Tomasi's polarizable continuum models). The results provide insight into the geometry and stability relations between the various  $\beta$ -turn subtypes. They show some characteristic deviations from the widely accepted standard rotation angles of  $\beta$  turns. The stability order of the  $\beta$ -turn subtypes depends strongly on the amino acid type. Thus, the replacement of L-amino acids in the two conformation-determining turn positions by D- or  $\alpha,\alpha$ -disubstituted amino acid residues generally increases the turn formation tendency and can be used to favor distinct  $\beta$ -turn subtypes in peptide and protein design. The  $\beta$ -turn subtype preferences, depending on amino acid structure modifications, can be well illustrated by molecular dynamics simulations in the gas phase and in aqueous solution. © 1997 by John Wiley & Sons, Inc. *J Comput Chem* **18**: 1415–1430, 1997

**Keywords:**  $\beta$  turns; peptide structure; peptide design; *ab initio* MO theory; theoretical conformational analysis; molecular dynamics

Dedicated to Prof. R. Borsdorf on the occasion of his 65th birthday and to Prof. P. Welzel on occasion of his 60th birthday.

Correspondence to: H.-J. Hofmann; e-mail: hofmann@rz.uni-leipzig.de

Contract/grant sponsor: Deutsche Forschungsgemeinschaft

Contract/grant sponsor: German Fonds der Chemischen Industrie

Contract/grant sponsor: Studienstiftung des Deutschen Volkes

Introduction

The three-dimensional structure of proteins is controlled by variation of the simplest elements of the secondary structure: helices,  $\beta$  sheets, and reverse turns. Among the reverse turns, the  $\beta$  turns play the most important role. They comprise about 25% of all residues in proteins<sup>1</sup> and occur mainly between two antiparallel  $\beta$  strands reversing the direction of the peptide chain.<sup>2,3</sup> The original definition of  $\beta$  turns considers them as a tetrapeptide segment consisting of the amino acid residues  $i$ ,  $i + 1$ ,  $i + 2$ , and  $i + 3$ .<sup>4</sup> These turns are differentiated by the backbone conformations of the residues  $i + 1$  and  $i + 2$ , represented by the torsion angles  $\varphi_{i+1}$ ,  $\psi_{i+1}$ ,  $\varphi_{i+2}$ ,  $\psi_{i+2}$ , whereas the terminal residues  $i$  and  $i + 3$  usually have  $\beta$ -strand main-chain conformations. The most widely used  $\beta$ -turn classification denotes six frequently occurring conformations as  $\beta$ I (common),  $\beta$ I' (inverse-common),  $\beta$ II (glycine),  $\beta$ II' (inverse-glycine),  $\beta$ III, and  $\beta$ III' turns, respectively.<sup>5,6</sup> These major types of  $\beta$  turns are indicated in numerous x-ray<sup>1,7-11,15</sup> and NMR studies.<sup>8,12,13</sup> Table I shows the widely accepted standard torsion angles for these conformations,<sup>4-11</sup> which were originally postulated by Venkatachalam<sup>4</sup> solely on the basis of theoretical considerations. Thus, these values are idealized and have to be proved by experimental data<sup>11</sup> and more elaborated theoretical methods.  $\beta$ III and  $\beta$ III' correspond to the first turn of a right- and left-handed  $3_{10}$ -helix, respectively, but the other turns of Table I also exhibit some relations to various helical conformations and are

sometimes considered as a combination of them.<sup>6</sup> A common feature of these  $\beta$  turns is the existence of a hydrogen bond between the main chain NH of the fourth amino acid ( $i + 3$ ) and CO of the first residue ( $i$ ), as shown in Figure 1, illustrating the common and glycine  $\beta$  turns together with their inverse counterparts. However, this hydrogen bond is not a necessary condition for  $\beta$ -turn formation. On the basis of two selection rules also arising from the analysis of x-ray protein data, namely the distance  $R$  between the  $C^\alpha$  atoms of the amino acid residues  $i$  and  $i + 3$ , which should be shorter than 7 Å,<sup>7,9,14</sup> and the torsion angle  $\tau$  formed by the  $C^\alpha$  atoms of the four turn amino acids, which should be in between  $-90^\circ \leq \tau \leq 90^\circ$ ,<sup>9,16</sup> Perczel et al. indicated 30 stable hairpin geometries in their systematic conformational analysis of the simple tetrapeptide model For—L-Ala—L-Ala—NH<sub>2</sub>, employing *ab initio* MO theory, and only a few of them were shown to exhibit a hydrogen bond as a stabilizing element.<sup>16</sup> However, most of these structures are relatively unstable and could only be expected sporadically in globular proteins in comparison to the above-mentioned major types of  $\beta$  turns.

A further interesting aspect of  $\beta$  turns appears when the amino acid L-proline occurs at position  $i + 2$ . Because of the higher percentage of cis peptide bonds that can be expected between proline and other amino acid residues, special  $\beta$  turns are formed with a cis peptide bond to the preceding amino acid, although a  $\beta$ I or at least a  $\beta$ III turn with proline in a trans peptide bond could still be possible from a geometrical point of view. These turns are denoted as  $\beta$ VIa and  $\beta$ VIb (Table I, Fig. 2),<sup>5,6</sup> respectively. The  $\beta$ VIa turn, but not the  $\beta$ VIb one, shows the above-mentioned hydrogen bond of the major types of  $\beta$  turns.

The reverse turns help to realize the compact structure of a globular protein. Moreover, the reverse turn motif may play an important role in recognition phenomena<sup>17-20</sup> and in the initiation of protein folding.<sup>21-23</sup> Both for a general understanding of the role of  $\beta$  turns in protein structures and for a rational design of peptide and protein mimetics by amino acid modification, knowledge of the structure and energetic relations between the major types of  $\beta$  turns seems necessary.<sup>24-27</sup>

Only a few quantum chemical studies on larger peptide units like  $\beta$  turns were performed employing semiempirical<sup>28</sup> and *ab initio* MO<sup>16,28-34</sup> methods. Interestingly, semiempirical methods like AM1 are not able to locate the  $\beta$ I turn as a

TABLE I. Standard Backbone Angles for the Major Types of  $\beta$  Turns.<sup>a, b</sup>

Turn	$\varphi_{i+1}$	$\psi_{i+1}$	$\varphi_{i+2}$	$\psi_{i+2}$
$\beta$ I	-60	-30	-90	0
$\beta$ I'	60	30	90	0
$\beta$ II	-60	120	80	0
$\beta$ II'	60	-120	-80	0
$\beta$ III	-60	-30	-60	-30
$\beta$ III'	60	30	60	30
$\beta$ VIa	-60	120	-90	0
$\beta$ VIb	-120	120	-60	0
$\beta$ VIb'	-120	120	-60	150

<sup>a</sup>Angles in degrees.  
<sup>b</sup>Refs. 4-11.

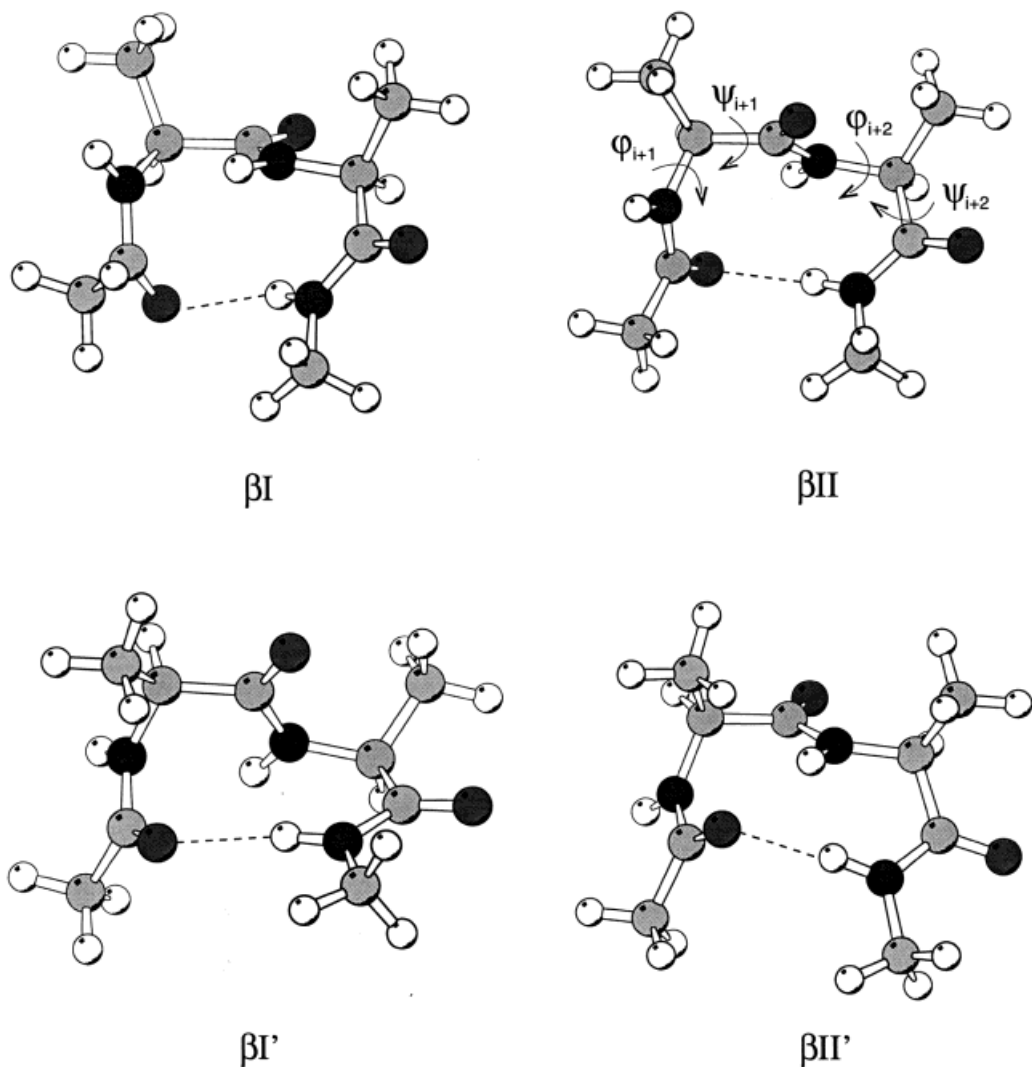


**FIGURE 1.** Common ( $\beta\text{I}$ ) and glycine ( $\beta\text{II}$ ) turns and their inverse counterparts  $\beta\text{I}'$  and  $\beta\text{II}'$ .

conformer in the  $\text{Ac-Gly-Gly-NHCH}_3$  model compound.<sup>28</sup> The scarce applications of *ab initio* MO theory concern only selected  $\beta$ -turn structures and are mostly at a relatively low basis set level with the exception of those previously mentioned. For a general understanding of  $\beta$  turns we refer the reader to the study by Perczel et al.,<sup>16</sup> working at the HF/3-21G level, and the study of Böhm,<sup>28</sup> who systematically examined the  $\beta\text{I}$  and  $\beta\text{II}$  turns of the  $\text{Ac-Gly-Gly-NHCH}_3$  model system in relation to some structural alternatives employing both the 3-21G basis set and a basis set of double-zeta quality supplemented by single-point MP2 correlation energy calculations.

Although the work of some investigators indicates the efficiency of the 3-21G basis set to repro-

duce essential features of peptide structures, some shortcomings become visible at this level. In particular, some profound studies on the diamides  $\text{For-L-Ala-NH}_2$  and  $\text{Ac-L-Ala-NHCH}_3$ , respectively, demonstrate the need of basis sets of higher quality and even the consideration of correlation energy to get quantitatively more reliable information on the structural and energetic characteristics of peptide conformations.<sup>35-40</sup>

It is one aim of this study, therefore, to present a systematic study on the major types of  $\beta$  turns at different basis set levels of *ab initio* MO theory and, in addition, estimate the influence of correlation energy, thermodynamic properties, and solvation on their structure and stability. These results may not only provide information on the efficiency

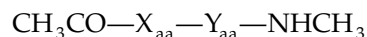
of the various approximation levels, but should also give a more detailed description of the relations between turn conformations than what is reflected by the data in Table I (i.e., referred to in papers and monographs). Moreover, considering that molecular mechanics will still be the most important tool for the treatment of larger peptides and proteins in the near future, these data could serve as reference for an improvement of empirical force fields, which, unfortunately, sometimes fail to reproduce correctly the major  $\beta$ -turn structures.<sup>28, 34, 41, 42</sup>

Apart from the general structural aspects of  $\beta$  turns being of interest, the consequences of special structure modifications of amino acids for the turn properties were examined. Such information could be helpful for peptide and protein design. Thus,  $\beta$  turns with the amino acids Gly and Ala were compared to estimate the influence of the prototype of an amino acid side-chain on the turn structures. Replacement of L-Ala by D-Ala served to describe possible changes induced by the alternate amino acid configurations. In this context, turns containing  $\alpha,\alpha$ -disubstituted amino acids were also considered with selection of  $\alpha$ -aminoisobutyric acid (Aib) as a model compound. Finally, the structures of the above-mentioned  $\beta$  VIa and  $\beta$  VIb turns with L-proline in the  $i + 2$  position were examined.

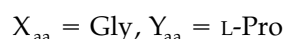
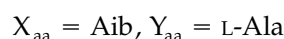
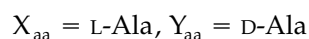
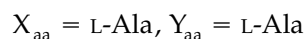
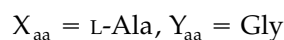
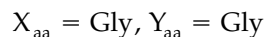
The general  $\beta$ -turn formation tendency and, in particular, the preference of one or the other  $\beta$ -turn subtype, depending on the various amino acid types, were also studied by employing molecular dynamics (MD).

## Methods of Calculations

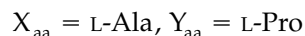
All  $\beta$  turns and related structures examined in this study can be derived from the general formula:



with



and



These model compounds represent prototypes well-suited to describe the essential structural principles of the major types of  $\beta$  turns and the possibilities of influence by structure modification. It should be mentioned that the  $\beta$ I/ $\beta$ I' and  $\beta$ II/ $\beta$ II' turns, respectively, are equivalent for  $\text{X}_{\text{aa}} = \text{Y}_{\text{aa}} = \text{Gly}$ . Remembering this fact, turn relations for configuration alternatives may be derived when knowing the results for one enantiomer; for example, the  $\beta$ I turn of  $\text{X}_{\text{aa}} = \text{L-Ala}$ ,  $\text{Y}_{\text{aa}} = \text{L-Ala}$  is energetically equivalent to the  $\beta$ I' turn of  $\text{X}_{\text{aa}} = \text{D-Ala}$ ,  $\text{Y}_{\text{aa}} = \text{D-Ala}$ , and the corresponding torsion

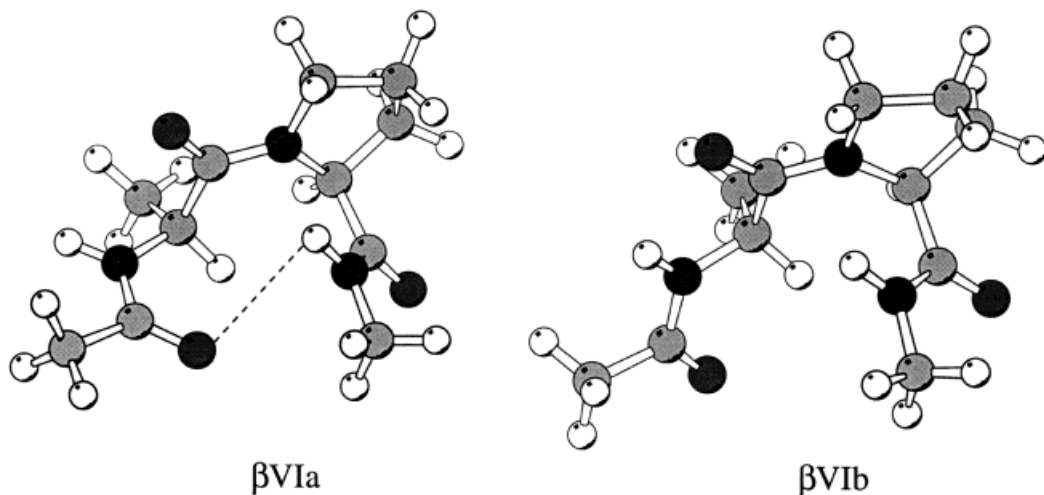


FIGURE 2.  $\beta$  VIa and  $\beta$  VIb L-proline turns.

angles differ only by sign. Thus, additional information could be gained from the results of the above-listed compounds.

Starting from the idealized conformations characterized by the angles in Table I, the geometries of all structures were completely optimized at the HF/6-31G\* and HF/3-21G levels of *ab initio* MO theory.<sup>43</sup> For the conformations of  $X_{aa} = Y_{aa} = \text{Gly}$ , it was possible to realize the geometry optimizations even at the MP2/6-31G\* level to determine the influence of the correlation energy. The Cartesian coordinates from these calculations are available on request. The MP2 correlation energies for all other structures were determined by single-point calculations based on HF/6-31G\* geometries. With exception of the proline model compounds, where the proline torsion angle  $\varphi$  is limited to about  $-60^\circ$ , extended conformations with main-chain rotation angles of  $180^\circ$  were also optimized to determine their exact rotation angles. Thus, the general turn formation tendency could be estimated in relation to these structures. The stationary points obtained in the optimizations were characterized by the determination of the eigenvalues of the force constants matrix. The HF/6-31G\* and HF/3-21G force constants, respectively, were used for the calculations of zero-point vibration energies, thermal energy, and entropy contributions, respectively. Sometimes,  $\beta\text{I}$  and  $\beta\text{I}'$  starting conformations changed into  $\beta\text{III}$  and  $\beta\text{III}'$  turns, respectively, and vice versa. In these cases, the potential hypersurface around the standard conformations was examined with special care to decide whether the  $\beta\text{I}$  ( $\beta\text{I}'$ ) and  $\beta\text{III}$  ( $\beta\text{III}'$ ) turns were excluding each other or could coexist. According to the standard torsion angles the  $\beta\text{I}$  ( $\beta\text{I}'$ ) and  $\beta\text{III}$  ( $\beta\text{III}'$ ) turns were close together. Thus, these conformations are possibly not distinct types.<sup>44</sup> Because of the importance of  $\beta\text{III}$  and  $\beta\text{III}'$  for the  $3_{10}$ -helix formation, it may be useful, therefore, to consider the two alternatives separately to enable an estimation of whether structure modifications more tend to  $\beta\text{I}/\beta\text{I}'$  turns or to right- and left-handed  $3_{10}$ -helices. Also, in some other cases, changes of the standard torsion angle values of one of the two amino acids determining the  $\beta$ -turn conformation into those of  $\beta$ -turn alternatives of Table I were observed. To confirm these changes, recalculations were performed where the standard values of the corresponding torsion angles were changed into the opposite direction of the observed optimization trend by at least  $10^\circ$  in the starting arrangements to reproduce these trends. Most of these situations concern the rela-

tion between the idealized torsion angles for  $\varphi_{i+2}$  and  $\psi_{i+2}$  in Table I and the typical values for these angles in a  $3_{10}$ -helix.

All quantum chemical calculations were performed employing the GAUSSIAN92 and GAUSSIAN94 program packages.<sup>45</sup> The optimizations were considered finished when all default criteria of these programs were fulfilled. In all our calculations the maximum residual force in Cartesian coordinates was distinctly below 0.001 mdyn at the end. For the estimation of the solvation influence on  $\beta$ -turn stability, two different quantum chemical continuum models were applied for comparison: the Onsager self-consistent reaction field (SCRF) model incorporated in the GAUSSIAN program packages, and the polarizable continuum model (PCM) developed by Tomasi and coworkers,<sup>46,47</sup> respectively. In the latter case, we used the original program from the Tomasi group at the University of Pisa, Italy. All solvation calculations were for the solvent water ( $\epsilon = 78.4$ ).

The MD simulations were performed for various model structures in the gas phase and in an aqueous environment employing the CHARMM 24b2 program package,<sup>48</sup> but using the CHARMM 23.1 force field<sup>49,50</sup> which is part of the QUANTA 4.1 modeling software.<sup>51</sup> The CHARMM force field describes relatively satisfactorily the starting conformations when comparing with the quantum chemical data. The gas phase simulations which provide information on the preferred conformation space arising from the actual molecular structure were realized following two strategies. On the one hand, trajectories of 1-ns time evolution were recorded after heating from 0 to 300 K and equilibration within 20 ps starting from the optimized extended forms of the model compounds. On the other hand, trajectories of 300-ps lengths were again generated after heating and equilibration, as before, but now starting from the optimized extended forms and the corresponding four optimized  $\beta$ -turn conformations I, I', II, and II', respectively. The time steps of integration were 1 fs, and the atom charges were calculated according to Gasteiger and Marsili.<sup>52</sup> All trajectories were first analyzed considering only the distance  $R$  between the  $\text{C}^\alpha$  atoms of the residues  $i$  and  $i + 3$  and all structures with  $R \leq 7 \text{ \AA}$  were accepted as  $\beta$  turns according to the general  $\beta$ -turn criterion mentioned earlier, which includes, of course, more  $\beta$ -turn conformations than the major types given in Table I. To focus on these major types, a second analysis of the trajectories additionally regarded the standard torsion angles to be fulfilled at the

**TABLE II.**  
**Relative Energies, Free Energies, and Dihedral Angles of Extended and  $\beta$ -Turn Conformations in Model Peptide Ac—Gly—Gly—NHMe.<sup>a</sup>**

Conf.	$\varphi_{i+1}$	$\psi_{i+1}$	$\varphi_{i+2}$	$\psi_{i+2}$	$\Delta E$	$\Delta G$	Method
Ext.	−171.2	−176.9	−179.7	−179.8	0.0 <sup>b</sup>	0.0	MP2/6-31G*
	180.0	180.0	179.7	−179.8	0.0 <sup>c</sup>	0.0	HF/6-31G*
	180.0	180.0	180.0	180.0	0.0 <sup>d</sup>	0.0	HF/3-21G
$\beta$ I	−72.1	−21.2	−99.6	15.3	−11.2	6.9 <sup>e</sup>	MP2/6-31G*
	−73.3	−17.7	−101.9	11.9	5.9	24.0	HF/6-31G*
	−67.8	−20.1	−108.2	19.7	1.1	9.4	HF/3-21G
$\beta$ II	−58.6	139.8	92.7	−14.0	−14.6	5.2 <sup>e</sup>	MP2/6-31G*
	−60.9	136.3	95.5	−11.7	1.2	21.0	HF/6-31G*
	−61.5	135.0	104.3	−21.2	−0.3	9.5	HF/3-21G

<sup>a</sup>Energies in kJ mol<sup>−1</sup>; angles in degrees.  
<sup>b</sup> $E_T = -662.542161$  a.u.  
<sup>c</sup> $E_T = -660.641395$  a.u.  
<sup>d</sup> $E_T = -656.955691$  a.u.  
<sup>e</sup> $\Delta G$  calculations are based on HF/6-31G\* thermochemical data.

same time within a range of  $\pm 50^\circ$ , which is generally applied in statistical analyses of  $\beta$  turns in protein structures.<sup>7</sup> The results from the five 300-ps trajectories were averaged and then compared with those from the 1-ns runs. The turn angle distributions arising from both strategies agree fairly well, thus demonstrating a sufficiently long period of

evolution for both procedures to get reliable information on the general conformation potential for  $\beta$ -turn formation and the preference of some subtypes in the gas phase.

For the MD simulation in aqueous solution, the extended forms were embedded into a cubic box of 25-Å size with 537 TIP3P water molecules. Peri-

**TABLE III.**  
**Relative Energies, Free Energies, and Dihedral Angles of Extended and  $\beta$ -Turn Conformations in Model Peptide Ac—L-Ala—L-Ala—NHMe.<sup>a</sup>**

Conf.	$\varphi_{i+1}$	$\psi_{i+1}$	$\varphi_{i+2}$	$\psi_{i+2}$	$\Delta E$	$\Delta G$	Method
Ext.	−156.6	160.4	−157.0	157.5	0.0 <sup>b</sup>	0.0	MP2/6-31G*//6-31G*
	−156.6	160.4	−157.0	157.5	0.0 <sup>c</sup>	0.0	HF/6-31G*
	−167.7	170.5	−167.7	169.8	0.0 <sup>d</sup>	0.0	HF/3-21G
$\beta$ I	−72.8	−18.9	−99.6	7.8	−5.8	7.1 <sup>e</sup>	MP2/6-31G*//6-31G*
	−72.8	−18.9	−99.6	7.8	3.8	16.7	HF/6-31G*
	−69.6	−17.1	−111.4	20.4	3.5	1.3	HF/3-21G
$\beta$ II	−60.2	133.7	66.5	20.0	−1.8	14.0 <sup>e</sup>	MP2/6-31G*//6-31G*
	−60.2	133.7	66.5	20.0	8.6	24.4	HF/6-31G*
	−69.2	106.5	66.3	29.7	9.6	12.7	HF/3-21G
$\beta$ I' ( $\beta$ III')	62.7	31.9	64.6	23.1	4.5	21.2 <sup>e</sup>	MP2/6-31G*//6-31G*
	62.7	31.9	64.6	23.1	19.5	36.2	HF/6-31G*
	61.1	28.9	63.9	21.4	11.1	16.9	HF/3-21G
$\beta$ II'	54.4	−132.2	−95.0	8.3	−1.7	15.4 <sup>e</sup>	MP2/6-31G*//6-31G*
	54.4	−132.2	−95.0	8.3	10.2	27.4	HF/6-31G*
	55.8	−131.1	−109.1	25.1	10.5	13.8	HF/3-21G

<sup>a</sup>Energies in kJ mol<sup>−1</sup>; angles in degrees.  
<sup>b</sup> $E_T = -740.878396$  a.u.  
<sup>c</sup> $E_T = -738.714689$  a.u.  
<sup>d</sup> $E_T = -734.605742$  a.u.  
<sup>e</sup> $\Delta G$  calculations are based on HF/6-31G\* thermochemical data.

odic boundaries, a cutoff radius of 12.0 Å for the nonbonded interactions, and SHAKE formalism keeping all XH bonds fixed were applied. The CHARMM template charges were selected for the solvation dynamics. After geometry optimization, heating from 0 to 300 K, and equilibration within 20 ps, trajectories of 2-ns length were registered and analyzed employing the same geometry criteria as given before. The integration time steps were again 1 fs in all cases. Several MD studies<sup>53–56</sup> on pentapeptides in aqueous solution generating trajectories over time intervals of 2 ns, and even 6.5 ns, demonstrate that protein folding initiation structures, like  $\beta$  turns, are formed and dissolved on the nanosecond time scale. The larger pentapeptides offer more structure alternatives than our smaller model systems. Thus, the time evolution of 2 ns should be sufficient to exhibit the main turn formation tendencies in our cases.

## Results and Discussion

### BASIC $\beta$ TURNS WITH GLYCINE AND L-ALANINE

In Tables II and III, the structural and energetic characteristics of the major types of  $\beta$  turns are presented for  $X_{aa} = Y_{aa} = \text{Gly}$  and  $X_{aa} = Y_{aa} = \text{L-Ala}$ , respectively, at various theoretical approximation levels. At first, the  $\beta$  turns with Gly in the  $i + 1$  and  $i + 2$  positions, where geometry optimizations up to the MP2/6-31G\* level were possible, should be regarded. At all three approximation levels (MP2/6-31G\*, HF/6-31G\*, HF/3-21G), the  $\beta\text{II}$  conformation is predicted to be more stable than the  $\beta\text{I}$  turn (Table II). Compared with protein structure data, the preference of  $\beta\text{II}$  over  $\beta\text{I}$  is particularly noteworthy in  $\beta$  turns with Gly in the  $i + 2$  position, thus the general term "glycine turn" is frequently used for  $\beta\text{II}$  conformations. In fact, when calculating the  $\beta\text{I}$  and  $\beta\text{II}$  turns for  $X_{aa} = \text{L-Ala}$ ,  $Y_{aa} = \text{Gly}$  at the HF/6-31G\* level, we also find the glycine turn by 6.2 kJ mol<sup>-1</sup> more stable than  $\beta\text{I}$ . Obviously, this relation is not changed by the side-chain of the L-amino acid in  $i + 1$  position provided that specific interactions with the peptide backbone can be excluded. Apart from the qualitatively satisfactory description of the stability order of the two turns at the various approximation levels, the quantitative agreement of the energetic data leaves something to be desired. The agreement between the HF/6-31G\*  $\beta\text{I}/\beta\text{II}$  energy difference of 4.7 kJ mol<sup>-1</sup> and the

MP2/6-31G\* value of 3.4 kJ mol<sup>-1</sup> is somewhat better than for HF/3-21G with 1.4 kJ mol<sup>-1</sup>. Comparable discrepancies are also confirmed by the results for the other  $\beta$ -turn model structures presented in the following paragraphs, even if the stability order of the various conformations agrees in all cases. Similar tendencies were already registered when comparing the results for some amino acid and diamide conformations obtained at the still higher HF/6-311G\* level with the corresponding MP2/6-311G\* data.<sup>40</sup>

The energetic relation between the two turn conformations and the extended form deserves a special comment. The extended conformation is more stable than the  $\beta$ -turns at the HF/6-31G\* level (Table II). However, this situation reverses when considering correlation energy. Obviously, the cyclic structures of the hydrogen-bonded turns are generally favored by correlation effects which is also confirmed by the results for the other model turns where at least the most stable  $\beta$  turn becomes more stable than the extended conformations and the other turns are relatively stabilized. A comparable effect becomes visible when calculating the energy difference between the so-called  $C_5$  and  $C_7$  conformations of For—L-Ala—NH<sub>2</sub>. Here, the  $C_5$  form resembles a more extended conformation ( $\varphi \approx -160^\circ$ ,  $\psi \approx 160^\circ$ ), whereas the  $C_7$  form represents a seven-membered hydrogen-bonded ring ( $\varphi \approx -85^\circ$ ,  $\psi \approx 75^\circ$ ). At the HF/6-311G\* level, the  $C_7$  ring is favored by 1.0 kJ mol<sup>-1</sup> and becomes still more stable with  $\Delta E = 6.5$  kJ mol<sup>-1</sup> after consideration of the MP2 correlation energy.<sup>40</sup> This phenomenon is reminiscent of comparable cases in other fields of structural chemistry; for instance, the relation between classical and nonclassical carbocations,<sup>58–60</sup> and the relation between the open and cyclic structure alternatives of trithiapentalene and its derivatives,<sup>61</sup> respectively, where only after consideration of correlation energy the preference of the cyclic structures is correctly reproduced. It would probably be rather difficult to consider such effects in an appropriate way when establishing empirical force fields for peptide structures. This could cause some problems when comparing different types of secondary structures.

Moreover, the situation becomes rather delicate when considering zero-point vibration energies and thermochemical data (Table II). Regarding now the relations between the extended form and the two  $\beta$ -turn conformations at the Gibbs free energy level, the original stability order found at the Hartree–Fock level is again established. Analyzing

these data in detail shows rather small effects coming from the zero-point vibration and thermal energies, but a considerable influence of the vibrational entropies destabilizing the cyclic turn conformations, probably because of their higher order. Thus, correlation energy effects and entropy contributions are compensating to a considerable extent. Therefore, the results at the HF/6-31G\* level may be considered a fair approximation for the free enthalpy differences between the various conformations, and, in addition, the relatively successful working of empirical force fields in the field of peptide and protein structures may be caused by partial compensation of correlation and entropy effects. Such aspects have to be considered when establishing or improving empirical force fields on the basis of different levels of *ab initio* MO theory and performing free energy calculations by means of molecular dynamics.

With respect to the agreement of the  $\beta$ -turn torsion angles obtained at the various approximation levels, the situation is quite satisfactory. Here, the MP2/6-31G\* and HF/6-31G\* values are close together, whereas the HF/3-21G torsion angles show larger deviations, but are still in an acceptable range. For  $X_{aa} = Y_{aa} = \text{Gly}$ , where only  $\beta\text{I}$  and  $\beta\text{II}$  are of interest, the calculated torsion angles listed in Table II agree quite well with the standard  $\beta$ -turn angles from Table I, but some interesting tendencies appear. Thus, the angle  $\varphi_{i+2}$  in  $\beta\text{I}$  is much closer to  $-100^\circ$  or even somewhat larger values than to the standard value of  $-90^\circ$ , respectively. Moreover, the torsion angle  $\psi_{i+2}$  deviates considerably from  $0^\circ$  and is closer to  $+20^\circ$  for  $\beta\text{I}$  and  $-20^\circ$  for  $\beta\text{II}$ . This corresponds more to several structure assignments in globular proteins.<sup>7,62</sup> Considerably larger values of  $>130^\circ$  compared with the standard value of  $120^\circ$  were calculated for the rotation angle  $\psi_{i+1}$  in the  $\beta\text{II}$  turn.

The essential difference when considering the  $\beta$  turns with alanine is the nonequivalence of the  $\beta\text{I}/\beta\text{I}'$  and  $\beta\text{II}/\beta\text{II}'$  turn pairs. The calculated stability order (Table III) found for the four turn conformations is  $\beta\text{I} > \beta\text{II} > \beta\text{II}' > \beta\text{I}'$  ( $\beta\text{III}'$ ) at all approximation levels (MP2/6-31G\*/6-31G\*, HF/6-31G\*, HF/3-21G). Again, the  $\beta$ -turn conformations are stabilized relatively to the extended form, which is most stable at the Hartree-Fock level, when considering correlation energy and again the same compensating effects between correlation energies and entropy contributions appear as discussed for the glycine turns. Even if solva-

tion is not included in our calculations, the stability orders on the basis of the HF/6-31G\* and the free enthalpy differences when including the correlation energies (Table III) may well be compared with those provided by free energy data from a molecular dynamics study in aqueous solution.<sup>24</sup> The higher stability of the  $\beta\text{I}$  turn, which was more unstable than  $\beta\text{II}$  in the turns with glycine, comes from a sterical hindrance between the side-chain of amino acid  $i + 2$  and the CO group of the preceding peptide bond in the  $\beta\text{II}$  conformation.

The inspection of the torsion angles of the  $\beta$  turns shows some new aspects. The  $\beta\text{I}$  and  $\beta\text{II}'$  turns formally correspond to the standard conformations when considering similar tendencies of angle increasing as was already found for glycine turns. However, in contrast to the glycine turns, the torsion angles  $\varphi_{i+2}$  and  $\psi_{i+2}$  in  $\beta\text{II}$  tend more to a left-handed  $3_{10}$ -helix ( $\beta\text{III}'$  turn) than to the  $\beta\text{II}$  standard values. Moreover, when starting the optimization from the  $\beta\text{III}$  standard angles, the  $\beta\text{I}$  turn results and starting from the  $\beta\text{I}'$  conformation provides the  $\beta\text{III}'$  turn. Thus, these small model peptide structures with L-amino acids do not realize the standard  $\beta\text{I}'$  and  $\beta\text{III}$  conformers, whereas  $\beta\text{I}$  and  $\beta\text{III}'$  represent minimum conformations. Confirmed by the results for the  $\beta$  turns of the other model compounds presented in the following paragraphs, it may be generalized that the  $\beta\text{I}'$  turn tends to  $\beta\text{III}'$  if the torsion angles of the  $\beta\text{I}$  conformation are closer to the standard values of Table I, if  $\beta\text{I}'$  better reflects the standard angles, the  $\beta\text{I}$  turn changes into  $\beta\text{III}$ . Similar conclusions can be drawn for the  $\beta\text{II}$  and  $\beta\text{II}'$  turns, but only concerning the amino acid residue  $i + 2$ .

Table IV provides information on some additional geometry parameters of selected  $\beta$  turns: the distance  $R$  between the  $\text{C}^\alpha$  atoms of the amino acids  $i$  and  $i + 3$ ; the torsion angle  $\tau$  formed by the four  $\text{C}^\alpha$  atoms of the amino acid residues; and the hydrogen bond characteristics, respectively, which are all in the expected range for  $\beta$ -turn conformations. The distances  $R$  are mostly between 5 and 6 Å, which is below the upper limit of 7 Å postulated for  $\beta$  turns.

#### INFLUENCE OF AMINO ACID CONFIGURATION ON $\beta$ -TURN STRUCTURES: $\beta$ TURNS WITH D-ALA AND AIB

As already discussed in the Methods section, the turn characteristics for one enantiomer could



**TABLE IV.**  
**Turn Characteristics  $R^a$  and  $\tau^b$  and Hydrogen Bond Features for  $\beta$  Turns of Model Peptides Ac—Gly—Gly—NHMe, Ac—L-Ala—L-Ala—NHMe, Ac—L-Ala—D-Ala—NHMe, Ac—L-Ala—L-Pro—NHMe, and Ac—Gly—L-Pro—NHMe.<sup>c</sup>**

$X_{aa}$	$Y_{aa}$	Turn	$R$	$\tau$	$R_{N \cdots O}$	$R_{N-H \cdots O}$	Method
Gly	Gly	$\beta I$	5.340	46.5	3.025	2.074	MP2/6-31G*
			5.687	48.8	3.247	2.294	HF/6-31G*
			5.264	43.3	3.049	2.086	HF/3-21G
		$\beta II$	5.448	32.0	3.007	2.032	MP2/6-31G*
			5.687	30.2	3.213	2.241	HF/6-31G*
			5.689	35.0	2.998	2.022	HF/3-21G
L-Ala	L-Ala	$\beta I$	5.665	50.7	3.215	2.260	HF/6-31G*
			5.258	43.8	3.051	2.092	HF/3-21G
			5.175	9.0	3.182	2.226	HF/6-31G*
		$\beta II$	4.658	-13.7	3.067	2.086	HF/3-21G
			6.061	-66.1	3.194	2.210	HF/6-31G*
			5.893	-68.3	3.009	2.022	HF/3-21G
		$\beta I'$	5.564	-27.6	3.128	2.160	HF/6-31G*
			5.689	-36.2	2.961	1.980	HF/3-21G
			6.132	70.2	3.269	2.287	HF/6-31G*
L-Ala	D-Ala	$\beta I$	5.987	73.7	3.069	2.083	HF/3-21G
			5.518	25.5	3.161	2.195	HF/6-31G*
			5.603	31.2	2.966	1.985	HF/3-21G
		$\beta II$	5.639	-47.4	3.149	2.185	HF/6-31G*
			5.105	-35.9	3.006	2.038	HF/3-21G
			5.192	-10.5	3.145	2.189	HF/6-31G*
		$\beta I'$	5.056	-8.3	2.943	1.998	HF/3-21G
			6.004	62.1	3.200	2.221	HF/6-31G*
			5.824	63.9	2.993	2.016	HF/3-21G
L-Ala	L-Pro	$\beta I$	5.783	44.0	3.044	2.257	HF/6-31G*
			5.731	38.2	2.867	1.944	HF/3-21G
			6.182	4.8	4.756	4.843	HF/6-31G*
		$\beta VIa$	6.527	7.5	5.036	5.158	HF/3-21G
			4.968	31.5	3.626	3.903	HF/6-31G*
			4.639	30.2	3.411	3.950	HF/3-21G
		$\beta VIb$	5.918	45.0	3.183	2.453	HF/6-31G*
			7.567	-103.1	5.089	4.958	HF/6-31G*

<sup>a</sup> $C^\alpha$  distance of the amino acids  $i$  and  $i + 3$ .

<sup>b</sup>Torsion angle between the  $C^\alpha$  atoms of the turn amino acids.

<sup>c</sup>Distances in angstroms; angles in degrees.

be used to get information on the turns of the other enantiomer, because any  $\beta$  turn of the one enantiomer represents the mirror image of that  $\beta$  turn of the other enantiomer whose torsion angles differ only by sign. Thus, the data for  $X_{aa} = Y_{aa} = D\text{-Ala}$  may immediately be derived from those for the  $X_{aa} = Y_{aa} = L\text{-Ala}$  system. Thus stability order for this model compound is  $\beta I' > \beta II' > \beta II > \beta I$  ( $\beta III$ ), and the geometry parameters of all complementary turns can be obtained simply by changing the sign of the torsion angles in Table III, which also shows that the  $\beta I$  standard turn now changes into the  $\beta III$  conformation. From these data it can

be concluded that the replacement of two consecutive L-amino acids in a peptide sequence, which usually support  $\beta I$  formation, by their D-enantiomers favors the formation of  $\beta I'$  turns. This rule could be useful for peptide and protein design.<sup>24</sup>

It may be interesting to examine the consequences of the replacement of only one L-amino acid by its D-enantiomer. In Table V, the results are given for the model compound  $X_{aa} = L\text{-Ala}$ ,  $Y_{aa} = D\text{-Ala}$ . It can be seen that the  $\beta II$  turn is the most stable conformation as it was found in the glycine turns. The steric interaction between the amino acid side-chain of the residue  $i + 2$  and the CO

**TABLE V.**  
**Relative Energies and Dihedral Angles of Extended and  $\beta$ -Turn Conformations in Model Peptide**  
**Ac—L-Ala—D-Ala—NHMe.<sup>a</sup>**

Conf.	$\varphi_{i+1}$	$\psi_{i+1}$	$\varphi_{i+2}$	$\psi_{i+2}$	$\Delta E$	Method
Ext.	−158.0	160.1	158.2	−159.4	0.0 <sup>b</sup>	MP2/6-31G*//6-31G*
	−158.0	160.1	158.2	−159.4	0.0 <sup>c</sup>	HF/6-31G*
	−167.7	170.9	167.7	−169.6	0.0 <sup>d</sup>	HF/3-21G
$\beta I$ ( $\beta III$ )	−70.6	−22.4	−64.8	−22.9	3.1	MP2/6-31G*//6-31G*
	−70.6	−22.4	−64.8	−22.9	15.3	HF/6-31G*
	−68.9	−18.0	−63.2	−22.9	12.3	HF/3-21G
$\beta II$	−61.4	131.5	94.4	−5.3	−10.0	MP2/6-31G*//6-31G*
	−61.4	131.5	94.4	−5.3	−1.7	HF/6-31G*
	−62.6	125.0	111.4	−20.3	−0.1	HF/3-21G
$\beta I'$	64.0	30.2	96.9	−7.0	−2.7	MP2/6-31G*//6-31G*
	64.0	30.2	96.9	−7.0	9.8	HF/6-31G*
	59.5	31.8	111.8	−24.8	2.3	HF/3-21G
$\beta II'$	54.2	−133.8	−66.6	−19.1	7.6	MP2/6-31G*//6-31G*
	54.2	−133.8	−66.6	−19.1	21.8	HF/6-31G*
	57.2	−132.5	−66.8	−17.1	21.3	HF/3-21G

<sup>a</sup>Energies in kJ mol<sup>−1</sup>; angles in degrees.  
<sup>b</sup> $E_T = -740.878572$  a.u.  
<sup>c</sup> $E_T = -738.714930$  a.u.  
<sup>d</sup> $E_T = -734.605773$  a.u.

group of the preceding peptide bond, which was responsible for the destabilization of  $\beta II$  in turns with L-amino acids, now concerns the  $\beta I$  turn. The determined stability order is  $\beta II > \beta I' > \beta I$  ( $\beta III$ )  $> \beta II'$ . This corresponds well again to the free energy data from MD simulations.<sup>24</sup> The conclusion for peptide design is the possibility of facilitating  $\beta II$  turn formation when replacing an L- with a D-amino acid in the  $i + 2$  position. The comparison of the energies of the turn conformations and the extended form shows that the introduction of a D-amino acid generally supports  $\beta$ -turn formation. Thus, the  $\beta II$  turn is more stable than the extended form already at the Hartree-Fock level. The torsion angles obtained for the various turns of this model system need no further comment and can well be understood when adequately transferring the comments already given for the other model systems.

The turn information for  $X_{aa} = \text{D-Ala}$ ,  $Y_{aa} = \text{L-Ala}$  follows immediately from the data of Table V when considering the above-mentioned enantiomer relations. Now, the stability order is  $\beta II' > \beta I > \beta I' (\beta III') > \beta II$ , which shows a favoring of  $\beta II'$  turns after a replacement of an L-amino acid in the  $i + 1$  turn position by the D-enantiomer. When considering a longer peptide sequence or a larger cyclopeptide with one L-amino acid replaced by its enantiomer, it cannot be concluded *a*

*priori* whether the D-amino acid prefers to enter the  $i + 1$  position forming a  $\beta II'$  turn then or position  $i + 2$  thus leading to a  $\beta II$  turn, because both turn possibilities are energetically equivalent. Which  $\beta$ -turn subtype finally forms depends on other factors; for instance, the other amino acids taking part in turn formation, solvation effects, and the ring size in cyclic peptides, respectively. However, it can be concluded from the energetic relations between the different  $\beta$ -turn subtypes of  $X_{aa} = Y_{aa} = \text{L-Ala}$  and  $X_{aa} = \text{L-Ala}$ ,  $Y_{aa} = \text{D-Ala}$  that  $\beta$ -turn formation involving the D-amino acid is generally favored over alternatives with only L-amino acids.

Numerous experimental studies indicate the  $\beta$  turn- and  $3_{10}$ -helix-inducing potency of  $\alpha,\alpha$ -disubstituted amino acids in peptide sequences.<sup>63–68</sup> Most results arise from peptide structures containing one or more residues of aminoisobutyric acid (Aib). If Aib enters the  $i + 2$  turn position, a  $\beta II$  turn results in most cases. Considering a model structure with  $X_{aa} = \text{L-Ala}$ ,  $Y_{aa} = \text{Aib}$ , competition between the turn formation tendencies supported by the structure elements  $X_{aa} = Y_{aa} = \text{L-Ala}$  tending to  $\beta I$  and  $X_{aa} = \text{L-Ala}$ ,  $Y_{aa} = \text{D-Ala}$  tending to  $\beta II$ , respectively, could be expected on the basis of our former conclusions. The results in Table VI show a preference of  $\beta II$  followed by  $\beta I (\beta III)$ ,  $\beta I' (\beta III')$ , and  $\beta II'$ . The higher stability of  $\beta II$

**TABLE VI.**  
**Relative Energies and Dihedral Angles of Extended and  $\beta$ -Turn Conformations in Model Peptides**  
**Ac—Aib—L-Ala—NHMe and Ac—L-Ala—Aib—NHMe at the HF/6-31G\* Level.<sup>a</sup>**

X <sub>aa</sub>	Y <sub>aa</sub>	Conf.	$\varphi_{i+1}$	$\psi_{i+1}$	$\varphi_{i+2}$	$\psi_{i+2}$	$\Delta E$
Aib	L-Ala	Ext.	−179.8	179.5	−157.4	159.9	0.0 <sup>b</sup>
		$\beta I$	−63.2	−29.5	−90.0	0.9	−0.4
		$\beta II$	−52.0	133.5	66.5	18.9	10.5
		$\beta I'$ ( $\beta III'$ )	61.9	31.6	64.7	23.6	9.7
		$\beta II'$	52.1	−132.3	−95.3	9.6	−0.3
		Ext.	−158.0	159.3	−178.9	−179.6	0.0 <sup>c</sup>
L-Ala	Aib	$\beta I$ ( $\beta III$ )	−70.3	−22.6	−61.8	−25.9	4.8
		$\beta II$	−60.4	134.4	63.8	22.8	−1.3
		$\beta I'$ ( $\beta III'$ )	62.5	32.3	62.1	25.6	9.7
		$\beta II'$	54.2	−133.7	−63.0	−23.6	11.4

<sup>a</sup>Energies in kJ mol<sup>−1</sup>; angles in degrees.

<sup>b</sup> $E_T = -777.746794$  a.u.

<sup>c</sup> $E_T = -777.746681$  a.u.

can be explained when remembering the results for the glycine turns, where this type predominates. Both missing of amino acid side-chains and, alternatively, a symmetrical disubstitution at the C $^\alpha$  atom of the  $i + 2$  amino acid residue favor quite obviously the  $\beta II$  over the  $\beta I$  turn. When placing the Aib residue in the  $i + 1$  position, competition between the  $\beta I$  and  $\beta II'$  turns should appear. This is in perfect agreement with the results of Table VI, indicating comparable stabilities for these two conformations followed by  $\beta I'$  ( $\beta III'$ ) and  $\beta II$ . The comparison of the stabilities of the turns with the corresponding extended forms shows an increased turn formation tendency in sequences with  $\alpha, \alpha$ -disubstituted amino acids. Again, at least the most stable turn is more stable than the extended conformation already at the Hartree–Fock level. No significant preference of the  $i + 1$  or  $i + 2$  turn position by Aib can be seen when comparing the total energies of the various  $\beta$ -turn conformations of the model compounds with Aib in the two different positions. The torsion angles of all  $\beta$ -turn subtypes in X<sub>aa</sub> = L-Ala, Y<sub>aa</sub> = Aib tend strongly to typical  $\beta III/\beta III'$  values, where possible, whereas the turns with Aib in the  $i + 1$  position fulfill the general rules discussed before. All these data may be useful for the estimation of structure influences on  $\beta$ -turn conformations by  $\alpha, \alpha$ -di-substituted amino acids dependent on the residue position. However, the basic structure effect on the selection of one or the other  $\beta$ -turn subtype comes from the different configuration. The design of a special  $\beta$ -turn subtype should

be better realized by the replacement of L- by D-amino acids and vice versa according to the rules derived above than by application of  $\alpha, \alpha$ -disubstituted amino acids where a second turn subtype always gains, or preferably keeps, considerable stability.

### STRUCTURE OF $\beta VIa$ AND $\beta VIb$ PROLINE TURNS

The peculiarities of the amino acid L-proline in  $\beta$ -turn formation are caused by the limited range of the torsion angle  $\varphi \approx -60^\circ$ , which concerns the rotation around a ring bond, and the higher percentage of cis peptide bonds formed between proline and other amino acids. In particular, when L-proline enters the  $i + 2$  position, special  $\beta$  turns with cis peptide bonds occur—which were mentioned previously in the Introduction section as  $\beta VIa$  and  $\beta VIb$ , respectively (Table I, Fig. 2). It may be interesting to compare the stabilities of these turns with that of the corresponding  $\beta I$  ( $\beta III$ ) turn with a trans peptide bond. Table VII provides the structural parameters and energies for the model systems X<sub>aa</sub> = L-Ala, Y<sub>aa</sub> = L-Pro and X<sub>aa</sub> = Gly, Y<sub>aa</sub> = L-Pro, respectively.

Two alternative possibilities were considered for the  $\beta VIb$  turn, because contradictory data of  $0^\circ$  and  $150^\circ$ , respectively, are given for the value of the  $\psi_{i+2}$  angle.<sup>5–8,13</sup> For differentiation of these two conformations, we denote the latter one as  $\beta VIb'$ . All calculations indicate the  $\beta VIa$  turn as most stable and the two cis turns more stable than the  $\beta I$  conformation, which tends to a  $\beta III$  turn.

**TABLE VII.**  
**Relative Energies and Corresponding Dihedral Angles of  $\beta$  Turns in the Model Peptides Ac—L-Ala—L-Pro—NHMe and Ac—Gly—L-Pro—NHMe.<sup>a</sup>**

Turn	$\varphi_{i+1}$	$\psi_{i+1}$	$\varphi_{i+2}$	$\psi_{i+2}$	$\Delta E$	Method
$X_{aa} = \text{L-Ala}, Y_{aa} = \text{L-Pro}$						
$\beta \text{I} (\beta \text{III})$	−61.7	−30.2	−69.9	−17.5	0.0 <sup>b</sup>	MP2/6-31G*//6-31G*
	−61.7	−30.2	−69.9	−17.5	0.0 <sup>c</sup>	HF/6-31G*
	−59.7	−27.2	−68.8	−16.4	0.0 <sup>d</sup>	HF/3-21G
$\beta \text{VIa}$	−61.0	146.2	−76.0	−14.3	−12.1	MP2/6-31G*//6-31G*
	−61.0	146.2	−76.0	−14.3	−12.4	HF/6-31G*
	−60.2	146.0	−90.8	21.6	−29.8	HF/3-21G
$\beta \text{VIb}$	−157.8	149.1	−71.4	−20.2	1.2	MP2/6-31G*//6-31G*
	−157.8	149.1	−71.4	−20.2	−5.5	HF/6-31G*
	−166.2	159.0	−69.0	−20.6	−5.7	HF/3-21G
$\beta \text{VIb}'$	−130.3	131.7	−50.2	159.4	−3.4	MP2/6-31G*//6-31G*
	−130.3	131.7	−50.2	159.4	−6.0	HF/6-31G*
	−124.7	128.4	−48.6	167.2	−6.2	HF/3-21G
$X_{aa} = \text{Gly}, Y_{aa} = \text{L-Pro}$						
$\beta \text{VIa}$	−65.8	153.6	−75.9	−13.1	0.0 <sup>e</sup>	HF/6-31G*
$\beta \text{VIb}'$	172.5	−167.8	−61.1	150.3	5.6	HF/6-31G*

<sup>a</sup>Energies in kJ mol<sup>−1</sup>; angles in degrees.  
<sup>b</sup> $E_T = -818.033619$  a.u.  
<sup>c</sup> $E_T = -815.605287$  a.u.  
<sup>d</sup> $E_T = -811.068163$  a.u.  
<sup>e</sup> $E_T = -776.573726$  a.u.

The  $\beta \text{VIb}$  and  $\beta \text{VIb}'$  conformations can both be localized as minimum structures of comparable stability. Thus, both arrangements could be expected in protein structures. Apart from some differences from the idealized values in Table I—in particular the distinctly larger values of the two torsion angles of amino acid  $i + 1$  in  $\beta \text{VIb}$  and of torsion angle  $\psi_{i+1}$  in  $\beta \text{VIa}$ —all turns fulfill the general geometry criteria with exception of the  $\beta \text{VIb} (\beta \text{VIb}')$  conformation with  $X_{aa} = \text{Gly}$ , where the torsion angles for the  $i + 1$  amino acid Gly tend strongly to the extended form. Thus, the distance and torsion angle criteria  $R$  and  $\tau$  are not fulfilled any longer and  $\beta \text{VIb} (\beta \text{VIb}')$  turns may be improbable for  $X_{aa} = \text{Gly}, Y_{aa} = \text{L-Pro}$  in peptide sequences (Tables IV and VII).

**SOLVENT INFLUENCE ON  $\beta$ -TURN STRUCTURES**

For the estimation of the influence of the solvent water on the various  $\beta$ -turn conformers employing the SCRF and the PCM formalisms, respectively, the model systems  $X_{aa} = Y_{aa} = \text{Gly}, X_{aa} = Y_{aa} = \text{L-Ala}$  and  $X_{aa} = \text{L-Ala}, Y_{aa} = \text{L-Pro}$  were selected.

Complete geometry optimization could be realized within the SCRF calculations, whereas the PCM results arise from single-point energy calculations based on HF/6-31G\* geometries. Because of the limitation of the dimension of the PCM program the proline turns could not be considered within this formalism and in the alanine turns the terminal methyl groups had to be replaced by hydrogens. The two continuum solvation models are based on numerous approximations. In particular, specific solute–solvent interactions could not be considered, which could be important for polar compounds like peptide structures. Thus, the results given in Table VIII should be considered mostly as a trend estimation of the solvent influence and their quantitative aspects should not be overestimated. Most striking is the strong solvent stabilization of the  $\beta \text{I}$  turn (also the  $\beta \text{I}'$  turn in the SCRF model) in relation to all other turn alternatives in L-amino acid sequences. This concerns all three model structures and is reflected by both solvation models. In the glycine and proline systems, the stability order is even reversed in favor of  $\beta \text{I}$ , and also, in the L-Ala models, the *a priori* preferred  $\beta \text{I}$  conformer gains additional stabiliza-

TABLE VIII.

Relative Solvation Energies, Free Energies, and Dihedral Angles of Extended and  $\beta$ -Turn Conformations of Model Peptides Ac—Gly—Gly—NHMe, Ac—L-Ala—L-Ala—NHMe, and Ac—L-Ala—L-Pro—NHMe at the HF/6-31G\* Level.<sup>a</sup>

X <sub>aa</sub>	Y <sub>aa</sub>	Conf.	$\varphi_{i+1}$	$\psi_{i+1}$	$\varphi_{i+2}$	$\psi_{i+2}$	$\Delta E$	$\Delta G$	Method
Gly	Gly	Ext.	179.6	180.0	-179.9	179.9	0.0 <sup>b</sup>		SCRF
			-179.4	179.3	179.1	-178.8		0.0 <sup>c</sup>	PCM
		$\beta$ I	-70.5	-20.5	-83.1	-6.2	-8.5		SCRF
			-73.3	-17.7	-101.9	11.9		-0.8	PCM
		$\beta$ II	-60.6	130.6	92.1	-8.8	-1.4		SCRF
			-60.9	136.3	95.5	-11.7		5.3	PCM
		Ala	-158.5	163.1	-157.4	162.7	0.0 <sup>d</sup>		SCRF
			-156.6	160.4	-157.0	157.5		0.0 <sup>e</sup>	PCM <sup>g</sup>
		$\beta$ I	-69.5	-22.7	-77.8	-12.6	-16.5		SCRF
			-72.8	-18.9	-99.6	7.8		-9.3	PCM <sup>g</sup>
Ala	Ala	$\beta$ II	-59.2	130.2	68.3	14.3	3.3		SCRF
			-60.2	133.7	66.5	20.0		6.7	PCM <sup>g</sup>
		$\beta$ I' ( $\beta$ III')	61.9	32.3	62.0	26.3	-1.3		SCRF
			62.7	31.9	64.6	23.1		5.3	PCM <sup>g</sup>
		$\beta$ II'	54.5	-128.1	-90.7	4.4	6.7		SCRF
			54.4	-132.2	-95.0	8.3		6.1	PCM <sup>g</sup>
		Ala	-60.4	-31.9	-68.2	-19.6	0.0 <sup>f</sup>		SCRF
			-60.9	146.0	-61.1	-3.4	12.0		SCRF
		$\beta$ VIb	-161.1	151.0	-69.4	-22.6	16.6		SCRF
			-131.3	132.9	-48.7	161.9	17.3		SCRF

<sup>a</sup>Energies in kJ mol<sup>-1</sup>; angles in degrees.

<sup>b</sup> $E_T = -660.646653$  a.u.

<sup>c</sup> $G_T = -660.675999$  a.u.

<sup>d</sup> $E_T = -738.718759$  a.u.

<sup>e</sup> $G_T = -660.522049$  a.u.

<sup>f</sup> $E_T = -815.615931$  a.u.

<sup>g</sup>The terminal methyl groups were replaced by hydrogens because of program dimension limitations.

tion in aqueous solution. Even if this effect is exaggerated, the general trend of the good solvent stabilization of  $\beta$ I seems to have some justification. Thus, the  $\beta$ I and  $\beta$ I' turns exhibit distinctly higher dipole moments than the other two subtypes, which may explain the Onsager SCRF results. The role of dipoles and dipole orientation in solvent stabilization of peptides has been pointed out by several investigators.<sup>26,53-56</sup> A recent study on  $\beta$  turns in aqueous solution confirms the general trend of solvent stabilization of  $\beta$ I turns.<sup>26</sup> It has even been concluded there that the  $\beta$ I turn gets its preference only by environmental effects. Even though the quantum chemical results unequivocally show the  $\beta$ I turn as the most stable turn conformation in L-amino acid peptide sequences in the gas phase also, this may underline the importance of solvation effects for its further stabilization. All solvation data may justifiably be transferred to amino acid sequences with D-amino acids.

The turn rotation angles determined in the SCRF optimizations confirm the essential tendencies found in the gas phase calculations. However, those for amino acid  $i+2$  are decreased in comparison to the gas phase values, thus now more closely resembling the standard values for the glycine and alanine turns.<sup>11</sup> The appearance of some differences between the conformer structures in the gas phase and in solution as indicated by our results deserves attention when developing force fields for the description of structures in the condensed phase.

### DYNAMICS OF $\beta$ -TURN SUBTYPE PREFERENCES

The quantum chemical results reflect rather well certain preferences of the major  $\beta$ -turn subtypes dependent on special amino acid structure modifications. It could be advantageous to study these phenomena from a dynamic point of view. There-

fore, molecular dynamics simulations were performed for the systems  $X_{aa} = Y_{aa} = \text{L-Ala}$ ;  $X_{aa} = \text{L-Ala}$ ,  $Y_{aa} = \text{D-Ala}$ ;  $X_{aa} = \text{L-Ala}$ ,  $Y_{aa} = \text{Aib}$ ; and  $X_{aa} = \text{Aib}$ ,  $Y_{aa} = \text{L-Ala}$ , respectively, to get both information on the general  $\beta$ -turn formation tendency and the preferences of the one or the other  $\beta$ -turn subtype in these systems. At first, it could be of interest to investigate the possibilities of structuring by gas phase simulations and then to examine whether these tendencies are maintained in aqueous solution.

On the basis of the two strategies described in the Methods section, several gas phase trajectories of 1-ns and 300-ps time evolution, respectively, were generated for the extended and  $\beta$ -turn conformations of the various model systems and subsequently analyzed. Quite comparable percentages, of about 35%, for the occurrence of  $\beta$ -turn conformations were found for the L-Ala turns when only considering the general  $\beta$ -turn distance criterion of  $R \leq 7 \text{ \AA}$ . The corresponding values for  $X_{aa} = \text{L-Ala}$ ,  $Y_{aa} = \text{D-Ala}$  and the two systems with Aib in the  $i + 1$  and  $i + 2$  position were 51%, 49%, and 57%, respectively, corresponding well to the increased  $\beta$ -turn formation tendency for sequences with D- or  $\alpha,\alpha$ -disubstituted amino acids already predicted by the quantum chemical data. These high percentages must not be identified with real turn frequencies in a peptide sequence. Also, other secondary structure types, in particular various helices, which are closely related to  $\beta$  turns anyway, fulfill this distance criterion. Thus, the data reflect a higher or lower  $\beta$ -turn formation potency in the various model structures which could be expected when they are part of or inserted into a peptide sequence. Whether turns, helices, or other secondary structure elements are finally formed in an actual amino acid sequence cannot be decided on the basis of these small model compounds.<sup>53–57</sup> In a second analysis, which additionally considered the angle criteria for the major  $\beta$ -turn types as given in Table I, and allowing for deviations of  $\pm 50^\circ$ , the  $\beta$ -turn occurrence decreased as expected. In Figure 3, the resulting distributions of the turn torsion angles, which had to be fulfilled at the same time to be selected as a turn conformation, are illustrated for the four model compounds. The  $\beta$ -turn subtype preferences became convincingly visible. Thus,  $\beta\text{I}$  predominates in  $X_{aa} = Y_{aa} = \text{L-Ala}$ .  $\beta\text{II}$  is strongly favored in  $X_{aa} = \text{L-Ala}$ ,  $Y_{aa} = \text{D-Ala}$ . For  $X_{aa} = \text{Aib}$ ,  $Y_{aa} = \text{L-Ala}$ , the equivalence of  $\beta\text{II}'$  and  $\beta\text{I}$ , and

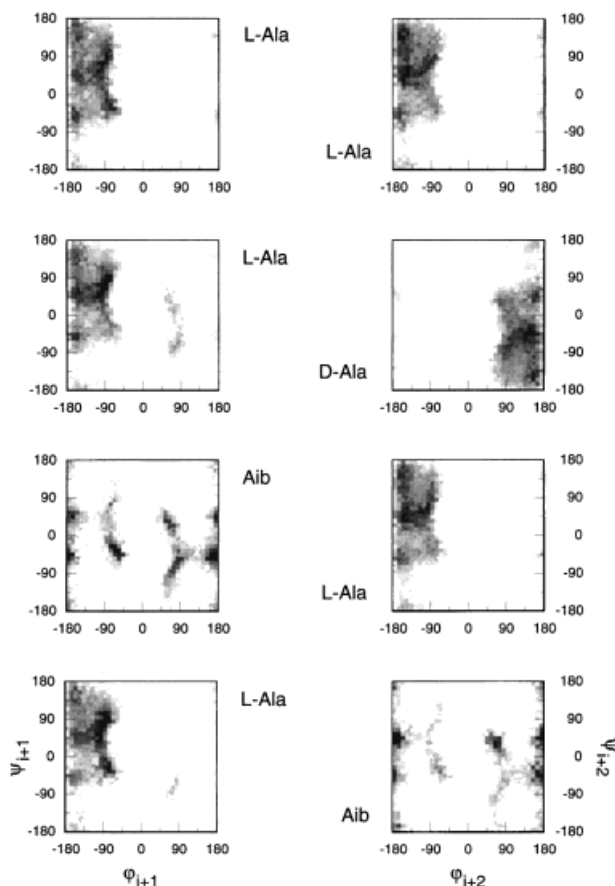


**FIGURE 3.** Turn angle distributions for various model  $\beta$  turns  $\text{Ac}-X_{aa}-Y_{aa}-\text{NHCH}_3$  from MD gas phase simulations.

for  $X_{aa} = \text{L-Ala}$ ,  $Y_{aa} = \text{Aib}$  the coexistence of  $\beta\text{II}$  and  $\beta\text{I}$  with  $\beta\text{II}$  higher populated are well reproduced. Analysis of the trajectories shows much higher conformational flexibility of the  $\psi$  than of the  $\varphi$  torsion angles of the amino acids  $i + 1$  and  $i + 2$  (Fig. 3).

Examining the dynamics of the extended forms of the various model structures in a water box of 25- $\text{\AA}$  size over 2 ns completely confirms these general trends. All  $\beta$ -turn formation tendencies found in the gas phase simulations are maintained and similar distributions of the torsion angles appear, as shown in Figure 3, even if a period of 2 ns may not yet be sufficient to reach the same quality of sampling as in the gas phase simulations, which becomes visible by longer periods of keeping particular  $\beta$ -turn structures formed in the simulations before changing into other conformations. This confirms the results from other MD studies<sup>53–56</sup> as already mentioned in the Methods section.

## Conclusions

The systematic analysis of the results of quantum chemical calculations on the various  $\beta$ -turn model compounds provides insight into the geometry and stability relations between the various turn subtypes, which should be considered when discussing structure problems of peptides and proteins involving  $\beta$  turns. The torsion angles, which show some characteristic differences in comparison with the widely accepted standard values, and also the stability order of the various  $\beta$ -turn subtypes, are strongly influenced by the amino acid structures. Thus, the replacement of an L-amino acid with a D- or  $\alpha,\alpha$ -disubstituted amino acid generally increases  $\beta$ -turn formation and favors distinct  $\beta$ -turn subtypes dependent on the position of variation in the sequence. Some general rules useful for the design of  $\beta$  turns in peptides and proteins are well supported by the quantum chemical and molecular dynamics results. Aqueous solvation favors, in particular, the  $\beta$ I turn in L-amino acid sequences. With L-proline in turn position  $i + 2$ , the  $\beta$ VIa turn, with a cis peptide bond to the preceding amino acid, gains considerable stabilization.

## Acknowledgments

We are obliged to Prof. M. Karplus, Harvard University, Cambridge, MA, and Prof. J. Tomasi, University of Pisa, Italy, for permitting use of the CHARMM and PCM program packages, respectively. Support of this work by Deutsche Forschungsgemeinschaft (Innovationskolleg Chemisches Signal und Biologische Antwort) and the German Fonds der Chemischen Industrie is gratefully acknowledged. One of us (M.G.) is obliged to Studienstiftung des Deutschen Volkes for a grant.

## References

1. W. Kabsch and C. Sanders, *Biopolymers*, **22**, 2577–2637 (1983).
2. E. J. Milner-White and R. Poet, *Trends Biochem. Sci.*, **12**, 189–192 (1987).
3. B. L. Sibanda and J. M. Thornton, *Nature (London)*, **316**, 170–174 (1985).
4. C. M. Venkatachalam, *Biopolymers*, **6**, 1425–1436 (1968).
5. J. Richardson, *Adv. Prot. Chem.*, **34**, 167–339 (1981).
6. J. S. Richardson and D. C. Richardson, In *Prediction of Protein Structure and the Principles of Protein Conformation*, G. Fasman, Ed., Plenum Press, New York, 1989, pp. 1–98.
7. P. Y. Chou and G. D. Fasman, *J. Mol. Biol.*, **115**, 135–175 (1977).
8. G. D. Rose, L. M. Gierasch, and J. A. Smith, *Adv. Prot. Chem.*, **37**, 1–109 (1985).
9. M. Levitt, *J. Mol. Biol.*, **104**, 59–107 (1976).
10. J. A. Smith and L. G. Pease, *Crit. Rev. Biochem.*, **8**, 315–399 (1980).
11. A. Perczel, I. Jakli, B. M. Foxman, G. D. Fasman, *Biopolymers*, **38**, 723–732 (1996).
12. H. J. Dyson, M. Rance, R. A. Houghten, R. A. Lerner, and P. A. Wright, *J. Mol. Biol.*, **201**, 161–200 (1988).
13. G. Müller, M. Gurrath, M. Kurz, and H. Kessler, *Prot. Struct. Funct. Genet.*, **15**, 235–251 (1993).
14. P. N. Lewis, F. A. Momany, and H. A. Scheraga, *Biochem. Biophys. Acta*, **303**, 211–229 (1973).
15. F. Richards and C. Kundrat, *Proteins*, **3**, 71–84 (1988).
16. A. Perczel, M. A. McAllister, P. Csaszar, and I. G. Csizmadia, *J. Am. Chem. Soc.*, **115**, 4849–4858 (1993).
17. R. L. Stanfield, T. M. Fieser, R. A. Lerner, and I. A. Wilson, *Science*, **248**, 712–719 (1990).
18. G. R. Marshall, *Curr. Opin. Struct. Biol.*, **2**, 904–919 (1992).
19. G. Nikiforovich and G. R. Marshall, *Int. J. Pept. Prot. Res.*, **42**, 171–180 (1993).
20. G. Nikiforovich and G. R. Marshall, *Int. J. Pept. Prot. Res.*, **42**, 181–188 (1993).
21. J. Scholnik and A. J. Kolinski, *J. Mol. Biol.*, **221**, 499–531 (1991).
22. K. V. Soman, A. Karini, and D. A. Case, *Biopolymers*, **31**, 1351–1361 (1991).
23. K. A. Dill, K. M. Fiebig, and H. S. Chan, *Proc. Natl. Acad. Sci. USA*, **90**, 1942–1946 (1993).
24. Y. Yan, B. W. Erickson, and A. Tropsha, *J. Am. Chem. Soc.*, **117**, 7592–7599 (1995).
25. D. K. Chalmers and G. R. Marshall, *J. Am. Chem. Soc.*, **117**, 5927–5937 (1995).
26. K. Ösapay, W. S. Young, C. Bashford, C. L. Brooks III, and D. A. Case, *J. Phys. Chem.*, **100**, 2698–2705 (1996).
27. H. Kessler, R. Gratias, G. Hessler, M. Gurrath, and G. Müller, *Pure Appl. Chem.*, **68**, 1201–1205 (1996).
28. H.-J. Böhm, *J. Am. Chem. Soc.*, **115**, 6152–6158 (1993).
29. A. Perczel, M. Kajtar, J. F. Maroccia, and I. G. Csizmadia, *J. Mol. Struct. (Theochem)*, **232**, 291–319 (1991).
30. D. B. Chesnut and C. G. Phung, *Chem. Phys. Lett.*, **183**, 505–509 (1991).
31. A.-M. Sapse, S. B. Daniels, and B. W. Erickson, *Tetrahedron*, **44**, 999–1006 (1988).
32. O. Antohi, F. Naider, and A.-M. Sapse, *J. Mol. Struct. (Theochem)*, **360**, 99–108 (1996).
33. L. Schäfer, S. Q. Newton, M. Cao, A. Peeters, C. Van Alsenoy, K. Wolinski, and F. A. Momany, *J. Am. Chem. Soc.*, **115**, 272–280 (1993).
34. C. Van Alsenoy, M. Cao, S. Q. Newton, B. Teppe, A. Perczel, I. G. Csizmadia, F. A. Momany, and L. Schäfer, *J. Mol. Struct. (Theochem)*, **286**, 149–163 (1993).

35. T. Head-Gordon, M. Head-Gordon, M. J. Frisch, C. Brooks, and J. A. Pople, *J. Am. Chem. Soc.*, **113**, 5389–5397 (1991).
36. I.R. Gould and P. A. Kollman, *J. Phys. Chem.*, **96**, 9255–9258 (1992).
37. H.-J. Böhm and S. Brode, *J. Am. Chem. Soc.*, **113**, 7129–7135 (1991).
38. K. Rommel-Möhle and H.-J. Hofmann, *J. Mol. Struct. (Theochem)*, **285**, 211–219 (1993).
39. I. R. Gould, W. D. Cornell, and I. H. Hillier, *J. Am. Chem. Soc.*, **116**, 9250–9256 (1994).
40. R. F. Frey, J. Coffin, S. Q. Newton, M. Ramek, V. K. W. Cheng, F. A. Momany, and L. Schäfer, *J. Am. Chem. Soc.*, **114**, 5369–5377 (1992).
41. S. S. Zimmermann and H. A. Scheraga, *Biopolymers*, **17**, 811–843 (1977).
42. S. S. Zimmermann and H. A. Scheraga, *Biopolymers*, **18**, 1849–1890 (1977).
43. W. J. Hehre, L. Radom, P. v. R. Schleyer, and J. A. Pople, *Ab Initio Molecular Orbital Theory*, Wiley, New York, 1986.
44. G. Nemethy and H. A. Scheraga, *Biochem. Biophys. Res. Commun.*, **95**, 320–327 (1980).
45. M. J. Frisch, G. W. Trucks, H. B. Schlegel, P. M. W. Gill, B. G. Johnson, M. A. Robb, J. R. Cheeseman, T. A. Keith, G. A. Peterson, J. A. Montgomery, K. Raghavachari, M. A. Al-Laham, V. G. Zakrzewski, J. V. Ortiz, J. B. Foresman, J. Cioslowski, B. B. Stefanov, A. Nanayakkara, V. Challcombe, C. Y. Peng, P. Y. Ayala, W. Chen, M. W. Wong, J. L. Andres, E. S. Replogle, R. Gomperts, R. L. Martin, D. J. Fox, J. S. Binkley, D. J. Defrees, J. Baker, J. P. Stewart, M. Head-Gordon, C. Gonzalez, and J. A. Pople, *GAUSSIAN 92*, 94 (Revision C.3), Gaussian, Inc., Pittsburgh, PA, 1995.
46. S. Miertus, E. Scrocco, and J. Tomasi, *J. Chem. Phys.*, **55**, 117–125 (1981).
47. J. L. Pascual-Ahair, E. Silla, J. Tomasi, and R. Bonaccorsi, *J. Comput. Chem.*, **8**, 778–787 (1987).
48. B. R. Brooks, R. E. Bruccoleri, B. D. Olafson, D. J. States, S. Swaminathan, and M. Karplus, *J. Comput. Chem.*, **4**, 187–217 (1983).
49. F. A. Momany and R. Rone, *J. Comput. Chem.*, **13**, 888–900 (1992).
50. F. A. Momany, R. Rone, H. Kunz, R. F. Frey, S. Q. Newton, and L. Schäfer, *J. Mol. Struct. (Theochem)*, **286**, 1–18 (1993).
51. *QUANTA, Version 4.1*, Molecular Simulations, Inc., 1994.
52. J. J. Gasteiger and M. Marsili, *Tetrahedron*, **36**, 3219–3228 (1980).
53. D. J. Tobias, J. E. Mertz, and C. L. Brooks III, *Biochemistry*, **30**, 6054–6058 (1990).
54. D. J. Tobias, S. F. Sneddon, and C. L. Brooks III, *J. Mol. Biol.*, **216**, 783–796 (1990).
55. C. L. Brooks III and D. A. Case, *Chem. Rev.*, **93**, 2487–2502 (1993).
56. D. J. Tobias, S. F. Sneddon, and C. L. Brooks III, In: *Advances in Biomolecular Simulations*, Vol. 239, R. Lavery, D. Rivail, and W. Smith, Eds., American Institute of Physics, Obernai, France, 1991, pp. 174–199.
57. A. Anderson and J. Hermans, *Proteins*, **3**, 262–265 (1988).
58. W. Koch, B. Liu, and D. J. DeFrees, *J. Am. Chem. Soc.*, **111**, 1527–1528 (1989).
59. K. Raghavachari, R. C. Haddon, P. v. R. Schleyer, and H. F. Schaefer III, *J. Am. Chem. Soc.*, **105**, 5915–5917 (1983).
60. M. Yoshimine, A. D. McLean, B. Liu, D. J. DeFrees, and J. S. Binkley, *J. Am. Chem. Soc.*, **105**, 6185–6186 (1983).
61. R. Cimiraglia and H.-J. Hofmann, *J. Am. Chem. Soc.*, **113**, 6449–6451 (1991).
62. C. M. Wilmot and J. M. Thornton, *Prot. Eng.*, **3**, 479–493 (1990).
63. E. Benedetti, *Biopolymers*, **40**, 3–44 (1996).
64. C. Toniolo, G. M. Bonora, A. Bavoso, E. Benedetti, B. Di Blasio, V. Pavone, and C. Pedone, *Biopolymers*, **22**, 205–215 (1983).
65. S. E. Huston and G. R. Marshall, *Biopolymers*, **34**, 75–90 (1994).
66. K. Okuyama and S. Ohuchi, *Biopolymers*, **40**, 85–103 (1996).
67. I. L. Karle, *Biopolymers*, **40**, 157–180 (1996).
68. E. E. Hodgkin, J. D. Clark, K. E. Miller, and G. R. Marshall, *Biopolymers*, **30**, 533–546 (1990).